We are IntechOpen,
the world's leading publisher of
Open Access books
Built by scientists, for scientists

6,900
Open access books available

186,000
International authors and editors

200M
Downloads

154
Countries delivered to

Our authors are among the

TOP 1%
most cited scientists

12.2%
Contributors from top 500 universities

CLARIVATE ANALYTICS

BOOK CITATION INDEX INDEXED

WEB OF SCIENCE™

Selection of our books indexed in the Book Citation Index
in Web of Science™ Core Collection (BKCI)

Interested in publishing with us?
Contact book.department@intechopen.com

Numbers displayed above are based on latest data collected.
For more information visit www.intechopen.com

Tuning the Morphology and Surface Property of Mineral Particles by Grinding Media

Zhiyong Gao and Chengwei Li

Additional information is available at the end of the chapter

Abstract

Grinding of minerals for particle size reduction and liberation is a prerequisite for successful mineral flotation separation and powder modification. Different grinding media produce mineral particles with different physical morphology and surface chemistry properties. Different mill particles expose different proportions of cleavage surfaces which lead to different shape indexes and different surface reactivities to organics, such as collector. Rod mill produces scheelite particles with a higher exposure of more reactive {101} surface that are beneficial for a stronger interaction with collector. More exposure of {101} surface also causes the rod mill particles to possess such values as larger elongation and flatness that are essential for particles attachment to air bubbles by shortening the induction time. The rod mill particles have a lower critical surface tension, greater hydrophobicity and a better flotation recovery when treated with the collector. In addition, the rod mill particles with a narrow particle size distribution have a smaller specific surface area, so the full monolayer adsorption of the collector on their surfaces can be achieved at a relatively lower concentration. These findings will help establish the relation between the particle surface physicochemistry and wettability, hence providing valuable guidance for the optimization of flotation separation and powder modification technology.

Keywords: grinding media, morphology, wettability, reactivity, flotation, surface modification, scheelite

1. Introduction

Size reduction by mechanical comminution (i.e., crushing and grinding) is an indispensable process in many fields, such as the field of mineral processing, metallurgical, power and chemical industries [1], etc. However, this process consumes such a considerable amount of energy that it becomes the heaviest energy consumption unit in many industries [2]. For

example, in the field of mineral processing, comminution of run-of-mine consumes 70% of the total energy [3]. Therefore, optimizing the process of crushing and grinding is of great significance for achieving energy-saving and cost-reducing in minerals processing.

Mineral processing is a predominant technology used to fulfill the enrichment of valuable minerals from coexisted (undesired) gangue minerals and then, provides raw materials for the following metallurgical operation [4]. During this process, minerals first go through crushing and grinding for particle size reduction and sufficient mineral liberation before separation operations [5, 6]. Conventionally speaking, there are primarily two ways for separation: gravity separation and flotation separation. Gravity separation is used when both the valuable minerals and gangues are coarsely grained in ore deposits and the density between them features a significant distinction. In this process, the rod mill is commonly employed to break preferentially coarser particles, produce more uniform particle products and avoid overgrinding [7–9]. In gravity separation, the valuable minerals and gangues have different movement speeds and trajectories in the equipment, such as jigging, dense medium cyclone and centrifuge, thus leading to the successful separation. But with the ever increasing demands for processing the low-grade, fine-grained and disseminated ores, the flotation separation has been increasingly employed as a complementary or substitute method for gravity separation [10]. Flotation is a separation method based on the differences in wettability at particle surfaces after being treated with surfactants, during which sufficient liberation of the fine-grained minerals is the key factor for a successful separation. Compared with the rod mill under the same energy consumption, the ball mill is more beneficial for the production of finer particle products [11].

Different grinding methods possess different breakage mechanisms and accordingly, produce particles with different shapes or morphologies [12]. For the rod mill, line loads are exerted on the mineral particles, and the predominant breaking forces are the impact which can produce particles with sharp edges [13]. In contrast, the ball mill imposes point loads on the particles, so that the main forces are abrasion and chipping which can trim off the corners and sharp edges of particles efficiently [14, 15]. Mill particles with different shapes always exhibit different gravity or flotation behavior. The research group led by Yekeler from Cumhuriyet University found that compared with the ball mill particles, the rod mill ones provide a more elongated and smoother surface, thus performing a better floatability [16–19]. This phenomenon can be explained by the higher attachment efficiency of the elongated particle to the air bubbles through accelerating the rupture of the surrounding liquid film and shortening the induction time [20, 21]. Recently, Xia [22] has systematically reviewed the role of particle shape in mineral floatability, and concluded that the particles with shape far away from sphere own an increasing surface hydrophobicity and floatability. Moreover, the coverage of collector on irregular particle surface is conducive to the stability of the three-phrase contact line and hence increasing the flotation recovery.

The grinding environments also play a considerable role on the surface properties and flotation behavior of the ground particles. Feng and Alrichv [23] indicated that more micro - structural defects found in the dry ground samples can serve as the active sites to accelerate the adsorption of collector, while smoother and cleaner surfaces are found in the wet mill particles. Recently, the spodumene samples were also ground using dry and wet mills by Zhu

et al. [24] and Xu et al. [25]. The separate research groups independently found that more {110} and {100} surfaces are exposed for the wet mill particles while more {010} exposed for the dry mill ones. The wet mill particles are more hydrophobic when treated with collector and accordingly, obtain a better flotation recovery.

Scheelite $CaWO_4$ is the most prominent mineral source for tungsten which is of great importance in many other fields like electronic information, aerospace and military [26]. The above two separation methods have been used to enrich the scheelite from gangue minerals for a long time [27–29]. In Xingluokeng Tungsten Ore (Fujian, China), the ore deposit mainly belongs to the scheelite-feldspar-quartz type. Because of the coarsely grained characteristics and distinct density differences between scheelite and gangues, the rod mill has been employed to achieve mineral liberation prior to the gravity separation. However, with the continuous consumption of the high-grade ore, the scheelite has become much more fine-grained. Thus, the gravity separation was proved to be less efficient in recent years, and a regrinding-flotation process after gravity separation was investigated to improve the comprehensive recovery of scheelite.

Unlike the Xingluokeng ore, the scheelite deposit in Shizhuyuan Ore (Hunan, China) mainly belongs to the scheelite-calcite-fluorite-grossularite type with a very fine-grained characteristic. Furthermore, due to the similar specific gravity between sheelite and grossularite, and similar physicochemical properties between scheelite and calcite and fluorite [30], the flotation method is therefore, the dominant process to recover the sheelite. Naturally, the ball mill is used to liberate the scheelite particles [31].

In the past 2 years, our group prepared a novel metal-organic complex, i.e., lead- benzohydroxamic acid (BHA) complex. This complex, as a collector, was successfully applied to the selective flotation of scheelite from gangues in Shizhuyuan Ore, leading to a significant increase in the comprehensive recovery of WO_3 by 8-10% [32, 33]. However, when we used this complex in Xingluokeng Ore, some obvious differences in the flotation behavior and recovery of scheelite were observed compared with those in Shizhuyuan Ore. We thought that the differences were mainly caused by the different mill media and ore type.

In this chapter, the surface properties and flotation behavior of scheelite particles produced by ball and rod mills were studied through single mineral flotation experiment, scanning electron microscopy (SEM) observation, wettability measurement, and X-ray diffraction (XRD) test. These results will help establish the relation between the particle surface properties and the grinding media, hence providing guidance for optimizing flotation separation.

2. Experimental procedures

2.1. Materials and reagents

Representative samples of pure scheelite crystals were collected from the Huili mine, Sichuan, China. The chemical analysis of samples confirmed that the scheelite samples were over 98% pure.

Chemically pure benzohydroxamic acid (BHA) (above 98% purity) was purchased from Tokyo Chemical Industry. Lead nitrate with 99% purity was purchased from Tianjin Kermil Chemical Reagents. The pH of solution was adjusted with sodium hydroxide (NaOH) or hydrochloric acid (HCl) stock solutions. Deionized (DI) water with a resistivity of over 18 M$\Omega \times$ cm was used throughout the experiments.

2.2. Methods

2.2.1. Grinding tests

Representative samples of pure scheelite crystal samples (**Figure 1a**) were first crushed from a diameter of 40–5 mm using the JC6 jaw crusher (Beijing Grinder Instrument Equipment Co., Ltd.). Then the crushed samples were ground by ball and rod mills. The grinding tests were operated using the 146 $\times$ 200 mm laboratory size mill (**Figure 1b**).

For the ball mill, corundum balls with diameters of 21, 16 and 12 mm were used as grinding media. For the rod mill, corundum rods of 15 and 11 mm in diameter and 15 cm in length were used. Scheelite samples with a total mass of 200 g were fed into the mill and ground for 30 s each run to prevent over-grinding. After a run, the ground products were sieved by a standard screen with a pore size of 74 μm (200 mesh). The oversize particles were returned to the mill for
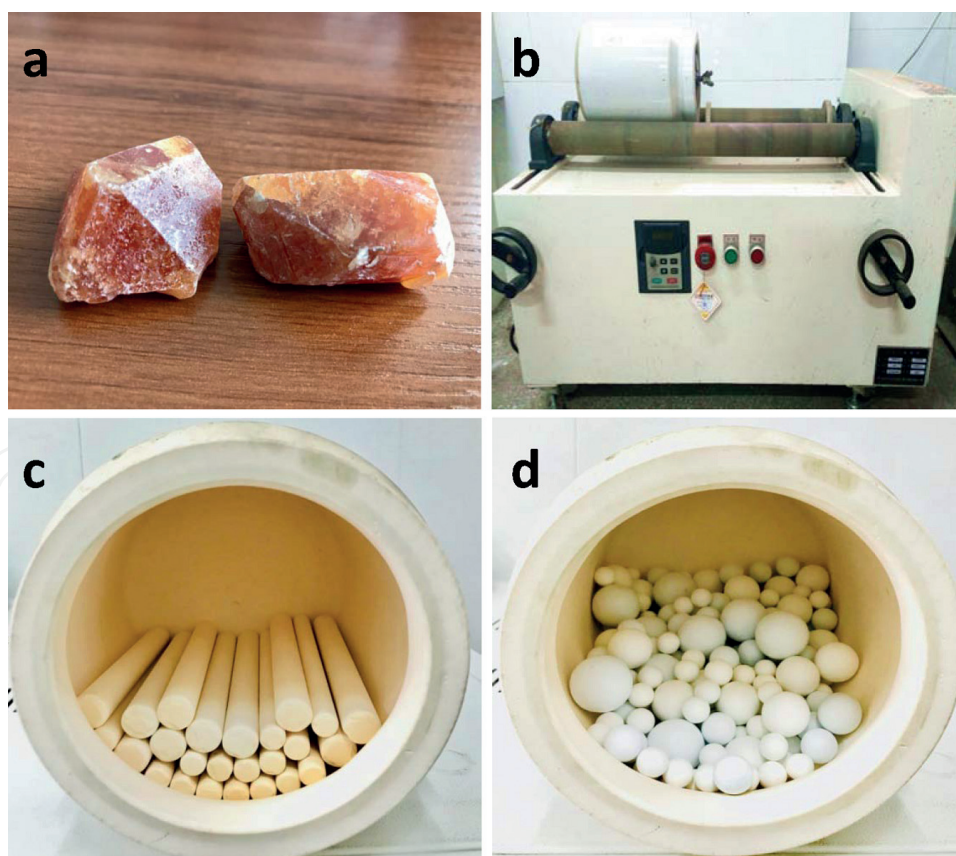

Figure 1. (a) Pure scheelite crystal samples, (b) grinder, (c) corundum rod media, and (d) corundum ball media used in the grinding tests.

the next run, while the products under the screen were collected for further sieving to obtain particles in the size fraction of $-74 + 38$ μm (the size of the particle is between 38 and 74 μm). The samples with required size were rinsed with Deionized (DI) water and dried at the temperature of 60°C. The surface area measurement (BET) indicated that the special surface areas of the ball and rod mill particles are 0.040 and 0.027 m^2/g, respectively.

2.2.2. Particle shape characterization by SEM

The shape characterization of milled particles was imaged by the JSM-6490LV SEM instrument. Assuming that the projection of the particles had the ellipse-like shape [17], the imaged micrographs were analyzed using CorelDraw×4 software to measure the length (L) and width (W) of the particles. As shown in **Figure 2**, the particles without overlapping nor border out of the picture were chosen. For each particle, the mean value of the five liner lengths and widths were taken as the real length (L) and width (W), respectively [16, 17]. Then more than 200 particles were measured and the L and W of the particle groups were calculated by averaging all value of the chosen particles.

Based on the ellipse-like shape assumption, Eqs. (1) and (2) were used to calculate the area (A) and perimeter (P), respectively.

$$A \approx \frac{\pi LW}{4} \tag{1}$$

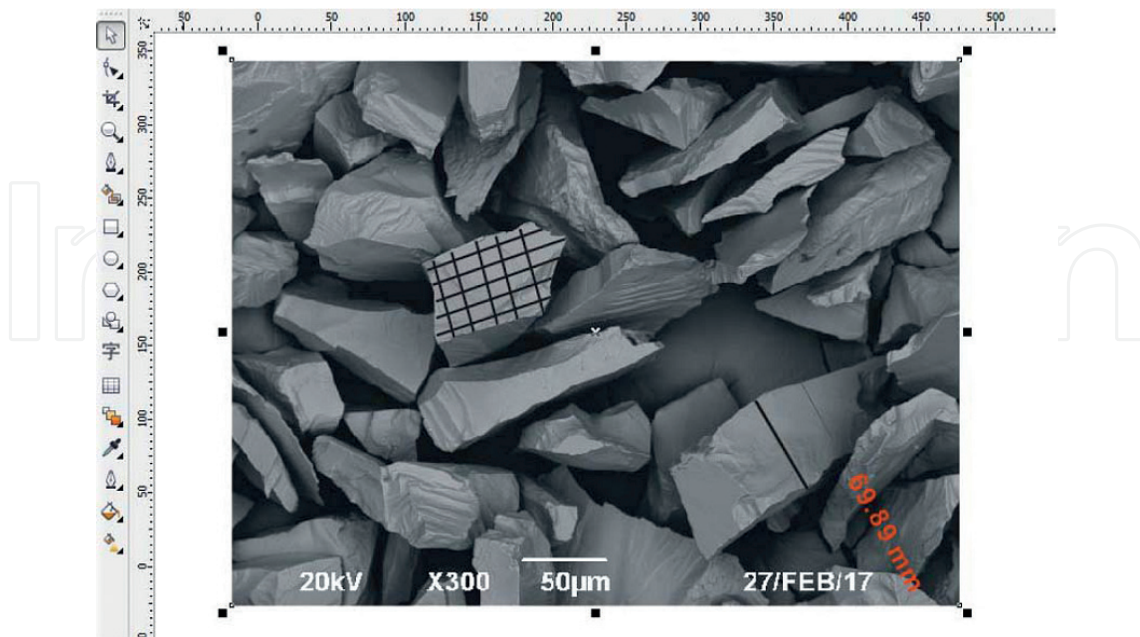$$P \approx \frac{1}{2}\pi\left[\frac{3}{2}(L + W) - (LW)^{1/2}\right] \tag{2}$$

Figure 2. Measurements of the length (L) and width (W) of a particle projection exported from an SEM micrograph on CorelDraw software.

With the values of L, W, A and P, the four shape factors, namely the roundness (Ro), flatness (F), elongation (E) and relative width (RW), were calculated using Eqs. (3)–(6).

$$Ro = \frac{4\pi A}{P^2} \tag{3}$$

$$F = \frac{P^2}{4\pi A} \tag{4}$$

$$E = \frac{L}{W} \tag{5}$$

$$RW = \frac{W}{L} \tag{6}$$

It should be noted that the maximum value of the roundness is 1.0 for a circle, while the flatness has a minimum of 1.0 for a circle.

2.2.3. X-ray diffraction (XRD) measurement

X-ray diffractometer (D8-ADVANCE Bruker-AKS) was run in the reflection mode with Cu Kαradiation (λ = 1.5406, tube potential of 40 mV, and tube current of 40 mA), and at a goniometer speed of 4°/min. It is important that the samples were randomly oriented during the sample preparation process.

2.2.4. Wettability measurement

To measure the wettability of nubby samples, the sessile drop technique [34] and the captive bubble method [35] have been widely used, while as for powder samples, the Washburn method [36] and the flotation method [37] were employed. In this study, the flotation method was employed to investigate the wettability of the milled particles treated by the activator and collector. This method is based on the assumption that the flotation recovery of the minerals decreases with the decrease in the surface tension (γ) of the solution [38]. Therefore, methanol solution with different concentrations were used as the flotation media and 2.0 g of samples was conditioned by 1×10^{-4} mol/L lead nitrate and 1×10^{-4} mol/L BHA. After 3 min of flotation at pH 9 (an industrially preferred pH for effective scheelite flotation), the froth concentrates and tailings were filtered, dried and weighted to calculate the flotation recovery.

Moreover, the advancing contact angle of the commonly exposed cleavage surfaces of scheelite (the {101} and {001} surfaces) was measured by the sessile-drop technology using a goniometer (GBX, France) at 20°C and ambient relative humidity of about 50%. The accuracy of the measurements was approximately ±2°. Firstly, and the prepared sample surfaces were immersed in the surfactant solution with desired concentration under gentle agitation for 30 min, then gently washed with distilled water and vacuum dried at 50°C for 15 min. Then a water drop of about 3.5 μL was placed on the sample surface and the readings of contact angles were taken automatically on the left and right sides of the water droplet profile by computer software. The height of the drop is dependent on the wettability of the scheelite

sample surface. Ten readings of contact angle were taken on each drop within 1 min after placing the drop, and the contact angle commonly reaches a stationary value (the equilibrium contact angle) after 30 s. At least three drops were measured and the mean value was taken as the real advancing contact angel for each crystal surface after treated with a certain concentration of collector [39–41].

2.2.5. Micro-flotation test

Micro-flotation tests were carried out in an XFG flotation machine with a 40 mL plexiglass cell, at an impeller speed of 1650 rpm. The mineral suspension was prepared by adding 2.0 g of minerals and 36 mL DI water into the flotation cell and agitated for 2 min, followed by the adjustment of pH using NaOH or HCl for 2 min. Then the reagents were added in following orders: (1) the lead nitrate as the activator (2) the BHA as the collector; (3) 25 μL/L (i.e., adding 25 μL frother into 1 L mineral suspension) terpineol as the frother. Once the desired reagent was added, the suspension was agitated for 3 min. The stable pH value was recorded before the flotation. The flotation process lasted for 3 min before the flotation products were collected, filtered, dried and weighted. The flotation recovery was calculated using the weight of the dry products.

3. Results and discussions

3.1. Shape indexes of scheelite particles by different mills

The shape characterization of both the ball and rod mill particles was determined using 2D shape analysis (SEM method), and the mean values of the main shape indexes calculated according to Eqs. (1)–(6) are listed in **Table 1**. In addition, the distribution of the roundness and the elongation were calculated and shown in **Figure 3**.

Furthermore, the Statistical Product and Service Solutions (SPSS) software and the "two-sample t-test" were applied to the study of shape index (flatness, roundness, elongation and relative width) differences of the products produced by the ball and rod mills. The values of the shape indexes were compared pair-wise for any statistically significant differences at the 95% confidence interval with the results listed in **Table 1**.

As shown in **Table 1**, the rod mill particles have higher values of elongation (E) and flatness (F), while the ball mill particles possess larger values of roundness (R) and relative width (RW). Since all values at the column of "Sig. (2-side)" listed in **Table 2** are less than 0.05, a significant difference between the ball and rod mill scheelite products with a confidence interval of 95% is

Mill products	Particle number	L(μm)	W(μm)	A(μm^2)	P(μm)	E	F	Ro	RW
Ball	240	96.140	63.830	4817.244	253.741	1.505	1.069	0.935	0.664
Rod	240	108.867	67.412	5796.279	281.199	1.615	1.097	0.916	0.623

Table 1. Mean values of the shape indexes of both the ball and rod mill products of the scheelite mineral.
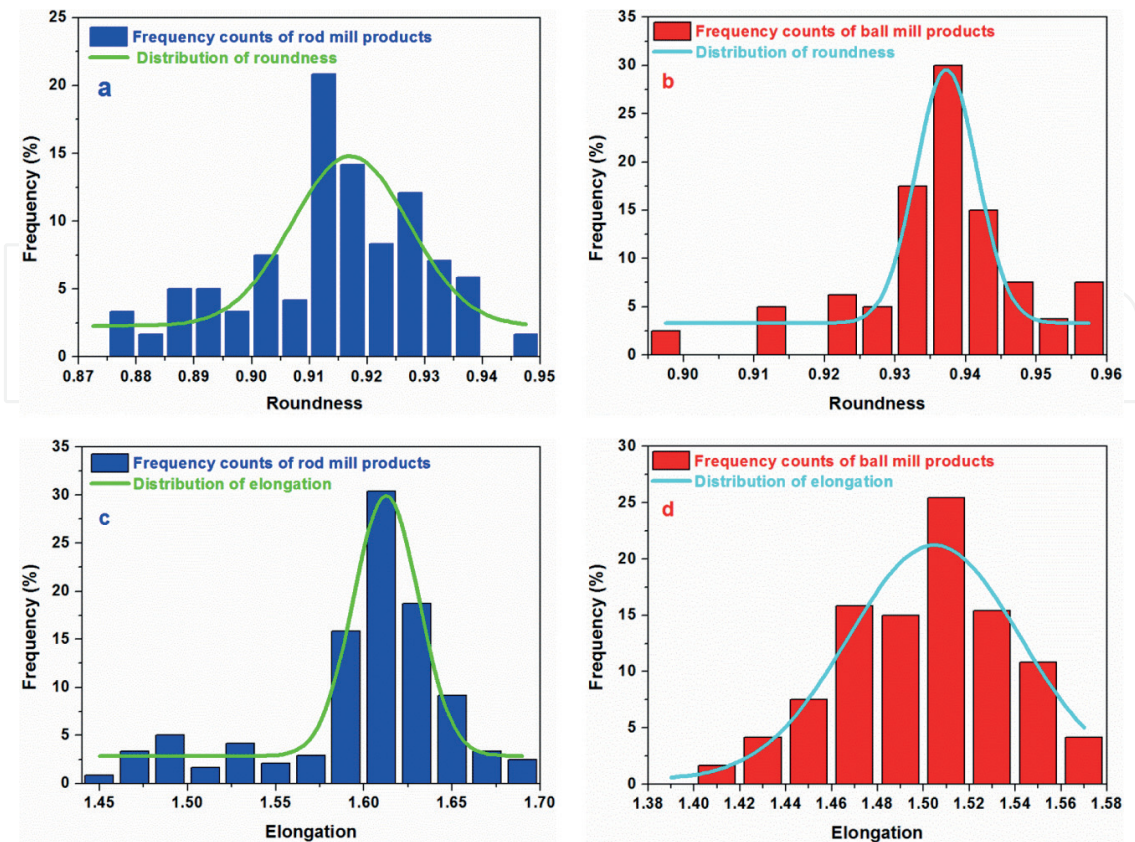
Figure 3. The distribution of shape indexes: The roundness of the (a) rod mill and (b) ball mill products, the elongation of the (c) rod mill and (d) ball mill products.

Parameter	Pair differences							
	Mean	Standard deviation	Standard error of mean	95% Confidence interval of the difference		t	df	Sig.(2-side)
				Lower	Upper			
F_d	0.02648	0.02363	0.00673	0.01614	0.03873	17.359	239	0.000
R_d	−0.02291	0.01986	0.00464	−0.0301	−0.0118	−17.555	239	0.000
E_d	0.10053	0.02021	0.00483	0.05160	0.14945	76.444	239	0.000
RW_d	−0.04127	0.00750	0.00222	−0.04910	−0.00886	−85.232	239	0.005

L_d, W_d, F_d, R_d, E_d and RW_d represent the shape differences of the scheelite particles produced by rod and ball mills.

Table 2. The statistical shape differences of the ball and rod mill products determined by the two-sample t-test.

inferred [42]. It was noted from the literature that the 2D shape data is used to reproduce the crucial shape characteristics of the real 3D shape indexes when the measured particles number is greater than 200 [43–47]. Therefore it is worth mentioning here that the shape indexes obtained in this study are reliable.
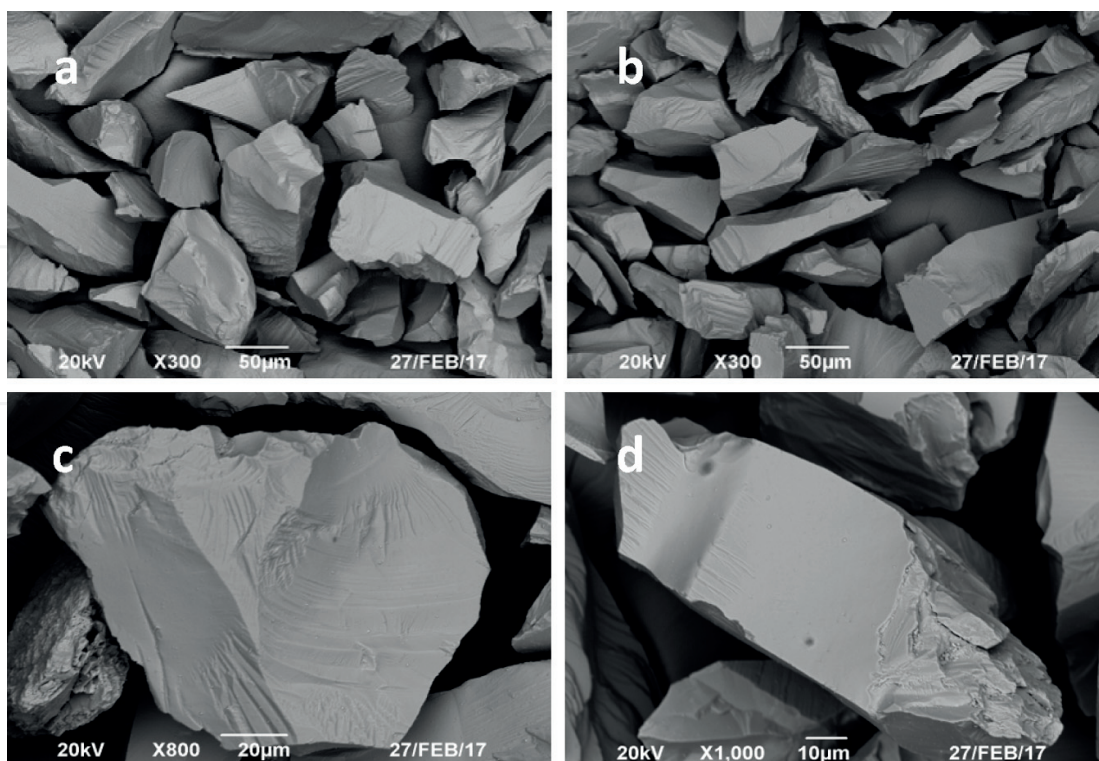
Figure 4. SEM pictures of the ball (a,c) and rod (b,d) mill particles of scheelite mineral.

SEM pictures in **Figure 4** show that the ball mill particles are more rounded while the rod mill particles are more elongated with more sharp edges. Those differences in the shape indexes between the ball and rod mill particles could be explained by the fact that breakage mechanism determines particle shape in all comminution equipment. The rod mill exercises line loads on the particles and the dominant breakage mechanism is the impact, during which the sharp edges are created, turning the particle to become more elongated [13]. Whereas the ball mill exerts point loads on the particles, and the predominant breaking forces are abrasion and chipping, which could eliminate the corners and sharp edges of the particles, turning them to become more rounded [14, 15].

3.2. XRD measurement results

Previous literatures reported that the relative exposure proportion of different crystal surfaces changes when the grinding environment varied [24, 25]. Previous publications revealed that the exposure of crystal surfaces of scheelite particles follows the order {112}, {101} and {001} [48–51]. The schematic of the commonly exposed surfaces of scheelite crystal particles can be found in **Figure 5**. In this work, the XRD measurements were conducted to investigate the exposure of different crystal surfaces in the two mill products, and the results are shown in **Figure 6**.

The relative intensity of a maxima (or peak) in the spectrum is believed to represent the relative exposure proportion of the crystal surfaces in the particulate samples [52, 53]. **Figure 6**
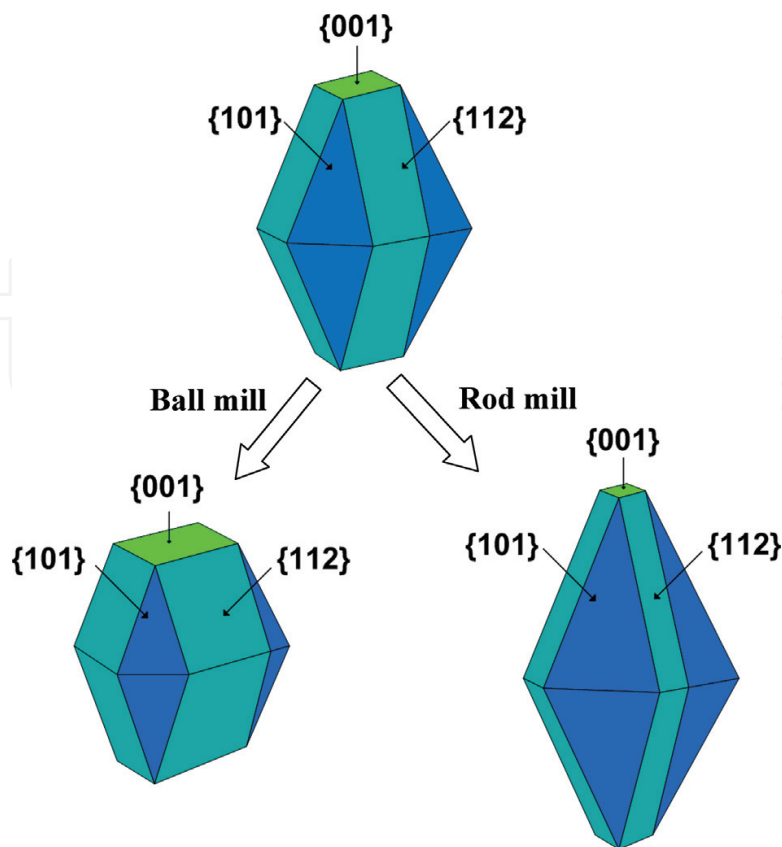
Figure 5. The schematic of the commonly exposed surfaces of original, ball and rod milled scheelite particles.

shows the same trend of the exposure of three main crystal surfaces of scheelite as **Figure 5**. Moreover, the {112} surface is the most abundant plane, and the intensity of the {112} surface is nearly the same for both mill products. In this case, the exposure proportion of {112} surface in the mill products is assumed as 100%. Accordingly, the relative proportions of the {101} plane in ball and rod mill samples are calculated to be 71.9% and 87.7%, respectively, while for the {001} planes, 44.4% and 33.8% respectively. The ball mill samples expose more {001} surfaces while the rod mill samples show more {101} surfaces. It is also interesting to mention that, from the **Figure 5**, more exposure of {001} surfaces will lead to the decrease in the elongation and the increase in the roundness of scheelite particles, while more exposure of {101} surface will increase the elongation and reduce the roundness of scheelite particles. That is to say, ball mill particles with more {001} surfaces are of a higher Ro value smaller E value which was verified by the results in **Table 1**.

It has been reported that every Ca atom on the scheelite {101} surface is fivefold-coordinated, while Ca on the {001} surface is sixfold-coordinated, as shown in **Figure 7**. The Ca atom in bulk scheelite crystal is eightfold-coordinated to surrounding oxygens. Based on our early findings [40, 54] that the atom with more dangling bonds is more active, the Ca atom on the {101} surface is more active than that on {001} surface, and has a higher interaction strength with organics, such as oleate. The atomic simulation results showed that a larger adsorption energy
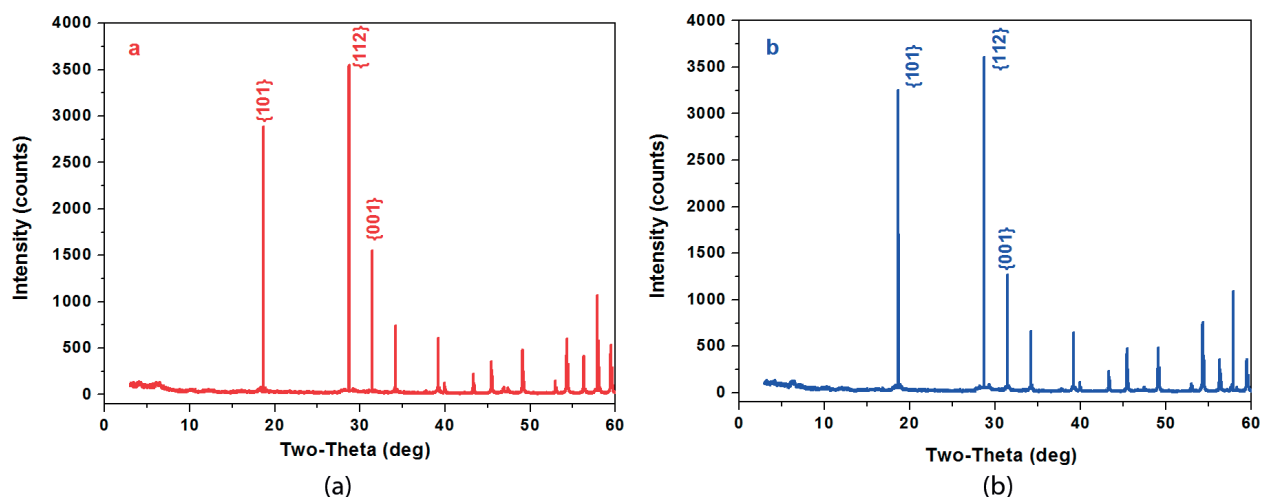
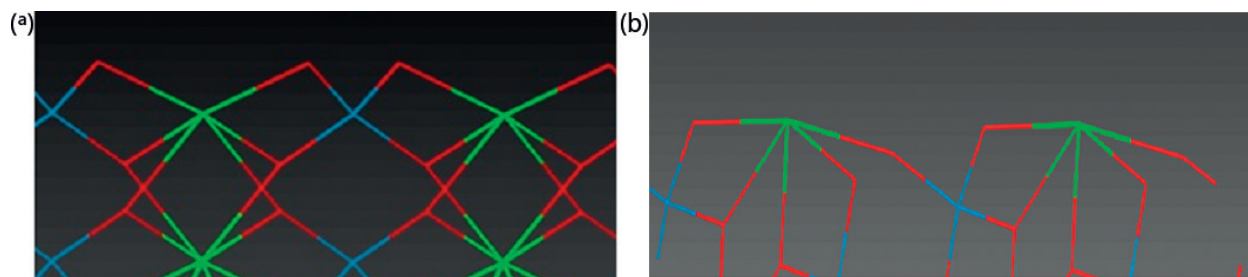**Figure 6.** The XRD spectrums of the (a) ball and (b) rod mill products of scheelite minerals.

Figure 7. The bonding state of the top layer of scheelite (a) {001} and (b) {101} surfaces (green-Ca, red-O, and blue-W).

(-102 kJ/mol) of the oleate on the {101} surface was calculated while the adsorption energy was -93 kJ/mol for the oleate on the {001} surface [10]. Thus, it is tenable to infer that the rod mill products with relatively more {101} surface have stronger interaction with the collector and may possess a higher flotation recovery.

3.3. Wettability test results

The flotation method was used to investigate the wettability of both ball and rod mill particles. The experiments were conducted at pH 9 using 1×10^{-4} mol/L lead nitrate as the activator and 1×10^{-4} mol/L BHA as the collector at different concentration of the methanol solution. The critical surface tension (γ_c) of wetting was determined by plotting the percent recovery (R%) versus the surface tension of the methanol - water solutions (γ_{LA}), which gives a recovery R% = 0 at $\gamma_c = \gamma_{LA}$. The particles are wetted and cannot float when $\gamma_{LA} < \gamma_c$, indicating that the mineral with a lower γ_c is more hydrophobic [55]. The γ_{LA} of the methanol solution was measured by the Automatic Surface Tensiometer and the results are provided in **Figure 8**. And the flotation results are shown in **Figure 9**. It shows that the γ_c of the ball and rod mill
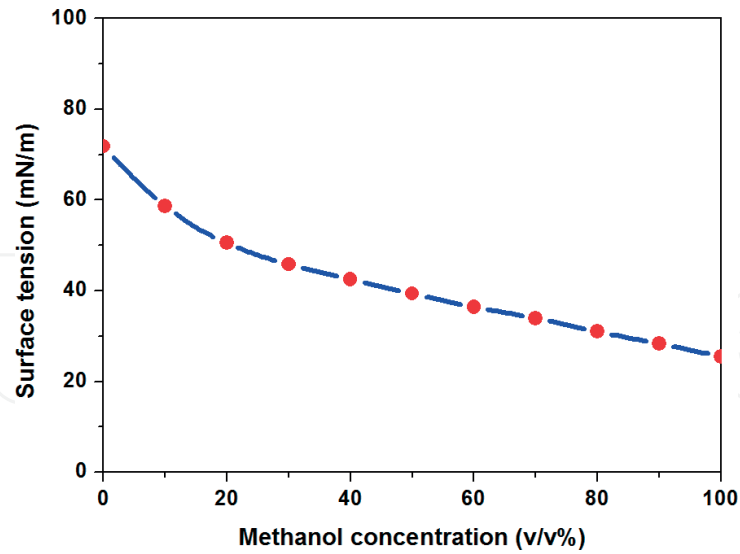
Figure 8. Variation of the surface tension of the methanol – water solutions (γ_{LA}) with the increase of mechanol concentration.

particles are approximately 43 and 41 mN/m, respectively, indicating that the ball mill ones are more likely to be wetted while the rod mill ones are more hydrophobic, which may result in a higher floatability.

According to the XRD measurement results, in addition to {112} surface, the ball mill samples expose more {001} surfaces while the rod mill samples show more {101} surfaces, which means that the wettability of the ground particles may be influenced by the proportion of the exposed surfaces. Then the advancing contact angles of both the {001} and {101} crystal planes treated by the lead nitrate and the BHA were measured, and the results are shown in **Figure 10**. It demonstrates that the scheelite {101} surface has higher contact angles after being treated with the surfactants, meaning that {101} is more hydrophobic than {001} surface.
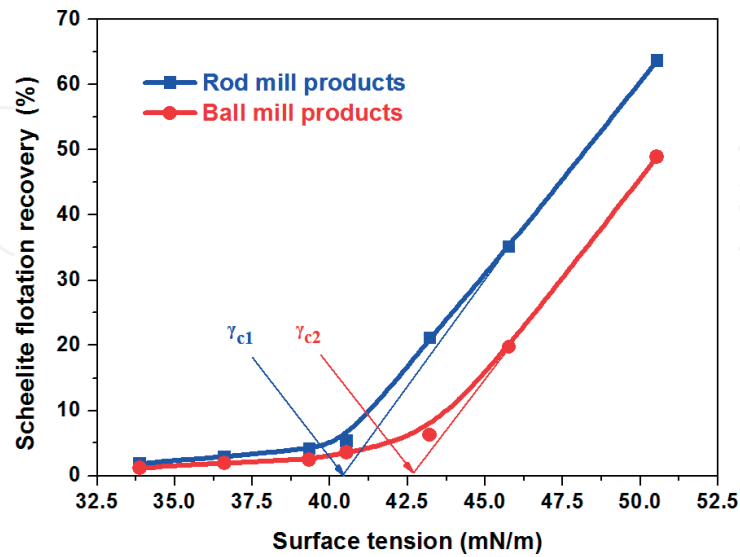

Figure 9. Flotation recoveries of the ball and rod mill products as a function of the methanol surface tension. ($C_{Lead\ nitrate} = 1 \times 10^{-4}$ mol/L; $C_{BHA} = 1 \times 10^{-4}$ mol/L; $C_{Terpineol} = 25$ μL/L; pH = 9 ± 0.2).

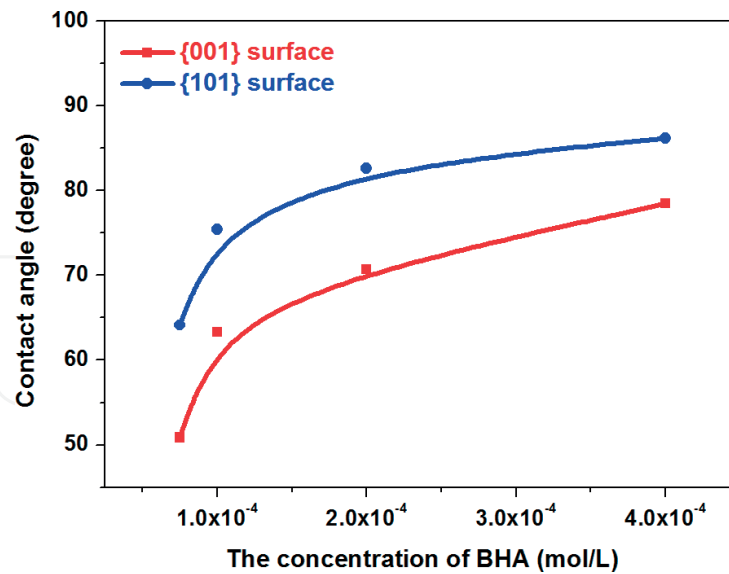**Figure 10.** Contact angles of the scheelite (a) {101} and (b) {001} crystal surfaces. ($C_{\text{Lead nitrate}} = 1 \times 10^{-4}$ mol/L; pH = 9 ± 0.2).

From the above measurements, it can be concluded that the rod mill particles with more {101} surfaces exposed and a lower critical surface tension were more hydrophobic. As a result, the differences in wettability could influence the flotation behavior of these two different mill particles.

3.4. Micro-flotation experiment results

Micro-flotation experiments were conducted to study the flotability of the particles in the fraction of −74 + 38 μm that ground by the ball and rod mills. The flotation results, using different concentrations of BHA as collector at a pH of 9 ± 0.2, are provided in **Figure 11**. **Figure 11** shows that both the ball and rod mill particles have a similar trend of flotation
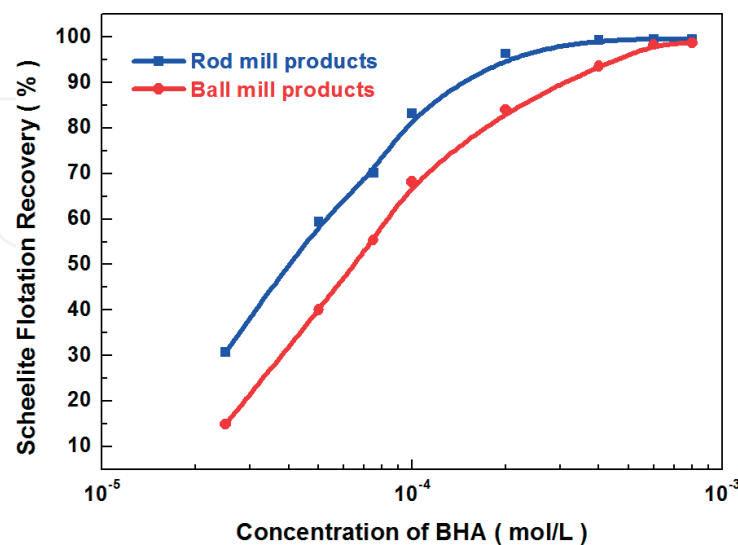

Figure 11. Flotation recoveries of the ball and rod mill products as a function of the BHA concentration. ($C_{\text{Lead nitrate}} = 1 \times 10^{-4}$ mol/L; $C_{\text{Terpineol}} = 25$ μL/L; pH = 9 ± 0.2).

recovery. The flotation recovery increases steadily with the increasing of BHA concentration till it reaches 4×10^{-4} mol/L for the rod mill particles and 6×10^{-4} mol/L for the ball mill ones, where the maximum recovery for both two samples are obtained at given concentrations of BHA, respectively. The maximum recovery may be caused by the monolayer adsorption of collector on the scheelite surfaces [56]. For the rod mill samples, it is easier to reach the monolayer adsorption because of the smaller specific surface area of 0.027 m²/g compared with that of 0.040 m²/g for the ball mill ones. Moreover, the flotation results, obtained at a pH of 6–11 are demonstrated in **Figure 12**. **Figure 12** shows that the recoveries of both milled particles follow a similar trend, but a higher recovery for the rod mill particles was observed. It was also observed that the flotation recovery increases with the increasing pH of solution until it reaches the value of 9, where the maximum recovery is achieved for both milled particles [32].

Therefore, it can be inferred from the micro-flotation results that the flotation behavior of the ball and rod mill particles is similar, while the rod mill ones have a better flotation performance than the ball mill ones. And the reason could be explained by the shape and the surface chemistry differences of scheelite particles ground by ball and rod mills. To begin with, the rod mill particles expose more {101} surfaces, on which the Ca sites are more reactive, resulting in a stronger interaction of collector with the rod mill particles and a better floatation performance. In addition, the wettability measurements show that the ball mill scheelite, with higher critical surface tension and more {001} surfaces, may have relatively lower contact angles and may be more likely to get wetted during the flotation process. Secondly, the rod mill particles, with a lower specific area and larger elongation, are more easily attached to the air bubbles than the rounded ones. This can be attributed to the sharp edges of elongated particles, which are conducive for rupturing the water film at the mineral/solution interface and help shorten the attachment time, leading to the improvement of the collision efficiency and flotation recovery.
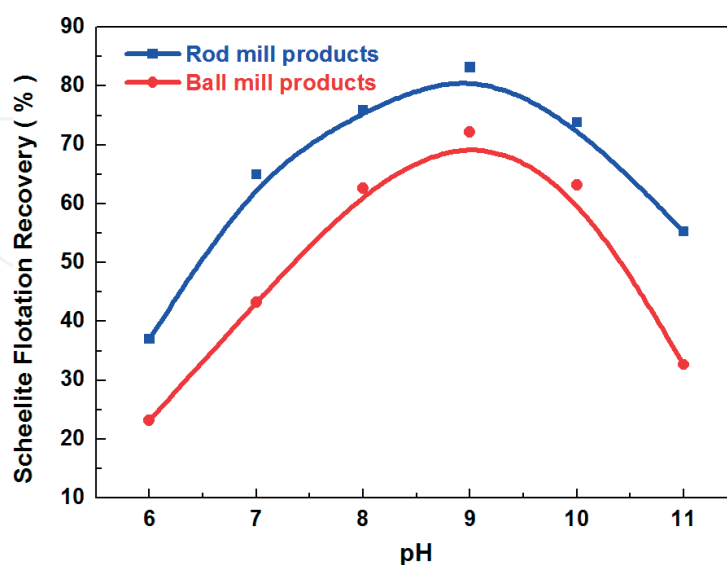

Figure 12. Flotation recoveries of the ball and rod mill products as a function of the solution pH. ($C_{\text{Lead nitrate}} = 1 \times 10^{-4}$ mol/L; $C_{\text{BHA}} = 1 \times 10^{-4}$ mol/L; $C_{\text{Terpineol}} = 25$ μl/L).

4. Conclusions

In this work, the morphology and the surface properties of the scheelite particles with a size of −74 + 38 μm produced by ball and rod mills were studied through SEM observation, XRD analysis, wettability measurement, and single mineral flotation experiment. The flotation results revealed that the rod mill particles are much easier to achieve a monolayer adsorption of collector and hence have a higher flotation recovery compared to the ball mill ones which can be explained from both physical and chemical points of view. The XRD spectrums showed that minerals particles obtained from ball and rod mill have similar expose intensity of abundant {112} surface. However, the rod mill particles have more {101} surface exposed with more reactive Ca atoms while more {001} surface is exposed for the ball mill particles. Moreover, more exposure of {001} surfaces will lead to the decrease in the elongation and the increase in the roundness of scheelite ball mill particles, while more exposure of {101} surface will increase the elongation and reduce the roundness of scheelite rod mill particles. Those discussions were verified by the SEM observations and shape indexes distribution calculation. The contact angles of {101} surface are larger than that of the {001} surface after being treated with the collector, indicating that the rod mill particles with more exposed {101} surfaces possess a higher hydrophobicity. The wettability measurements indicated that the values of the critical surface tension (γ_c, a measure of surface tension) are 41 and 43 mN/m for the rod and ball mill particles treated with collector, respectively. The rod mill particles with more exposure of reactive {101} surfaces and higher elongation have stronger attachment to collectors and air bubbles, and hence a higher hydrophobicity and flotation recovery in the presence of collector.

Acknowledgements

Author details

Zhiyong Gao* and Chengwei Li

*Address all correspondence to: zhiyong.gao@csu.edu.cn

School of Mineral Processing and Bioengineering, Central South University, Changsha, Hunan, China

References

[1] Kursun H, Ulusoy U. Influence of shape characteristics of talc mineral on the column flotation behavior. International Journal of Mineral Processing. 2006;**78**:262-268. DOI: 10.1016/j.minpro.2005.11.003

[2] Ballantyne GR, Powell MS. Benchmarking comminution energy consumption for the processing of copper and gold ores. Minerals Engineering. 2014;**65**:109-114. DOI: 10.1016/j.mineng.2014.05.017

[3] Curry JA, Ismay MJL, Jameson GJ. Mine operating costs and the potential impacts of energy and grinding. Minerals Engineering. 2014;**56**:70-80. DOI: 10.1016/j.mineng.2013.10.020

[4] Austin LG, Trass O. Size reduction of solids crushing and grinding equipment. In: Fayed ME, Otten L, editors. Handbook of Powder Science & Technology. Boston, MA: Springer US; 1997. pp. 586-634

[5] Leroy S, Dislaire G, Bastin D, Pirard E. Optical analysis of particle size and chromite liberation from pulp samples of a UG2 ore regrinding circuit. Minerals Engineering. 2011;**24**:1340-1347. DOI: 10.1016/j.mineng.2011.06.006

[6] Bournival G, Ata S, Wanless EJ. The roles of particles in multiphase processes: Particles on bubble surfaces. Advances in Colloid and Interface Science. 2015;**225**:114-133. DOI: 10.1016/j.cis.2015.08.008

[7] Abouzeid AZM, Fuerstenau DW. Flow of materials in rod mills as compared to ball mills in dry systems. International Journal of Mineral Processing. 2012;**102**:51-57. DOI: 10.1016/j.minpro.2011.09.013

[8] Heyes GW, Kelsall DF, Stewart PSB. Continuous grinding in a small wet rod mill part I. Comparison with a small ball mill. Powder Technology. 1973;**7**:319-325. DOI: 10.1016/0032-5910(73)80043-9

[9] Tavares LM, de Carvalho RM, Guerrero JC. Simulating the bond rod mill grindability test. Minerals Engineering. 2012;**26**:99-101. DOI: 10.1016/j.mineng.2011.10.015

[10] Cooper TG, de Leeuw NH. A computer modeling study of the competitive adsorption of water and organic surfactants at surfaces of the mineral scheelite. Langmuir. 2004;**20**:3984-3994. DOI: 10.1021/la049796w

[11] Oja M, Tuunila R. The influence of comminution method to particle shape. In: Massacci P, editor. Developments in Mineral Processing. Elsevier; 2000. p. C4-64-C64-70. DOI: 10.1016/S0167-4528(00)80028-9

[12] Moosakazemi F, Mohammadi MRT, Mohseni M, Karamoozian M, Zakeri M. Effect of design and operational parameters on particle morphology in ball mills. International Journal of Mineral Processing. 2017;**165**:41-49. DOI: 10.1016/j.minpro.2017.06.001

[13] Ulusoy U, Yekeler M. Correlation of the surface roughness of some industrial minerals with their wettability parameters. Chemical Engineering and Processing. 2005;**44**:557-565. DOI: 10.1016/j.cep.2004.08.001

[14] Vizcarra TG, Wightman EM, Johnson NW, Manlapig EV. The effect of breakage method on the shape properties of an iron-oxide hosted copper-gold ore. Minerals Engineering. 2011;**24**:1454-1458. DOI: 10.1016/j.mineng.2011.07.007

[15] Francioli D. Effect of operational variables on ball milling. Tijdschrift Voor Theologie. 2015;**52**:180-180

[16] Hicyilmaz C, Ulusoy U, Yekeler M. Effects of the shape properties of talc and quartz particles on the wettability based separation processes. Applied Surface Science. 2004;**233**: 204-212. DOI: 10.1016/j.apsusc..2004.03.209

[17] Yekeler M, Ulusoy U, Hicyilmaz C. Effect of particle shape and roughness of talc mineral ground by different mills on the wettability and floatability. Powder Technology. 2004; **140**:68-78. DOI: 10.1016/j.powtec.2003.12.012

[18] Ulusoy U, Hicyilmaz C, Yekeler M. Role of shape properties of calcite and barite particles on apparent hydrophobicity. Chemical Engineering and Processing. 2004;**43**:1047-1053. DOI: 10.1016/j.cep.2003.10.003

[19] Ulusoy U, Yekeler M, Hicyilmaz C. Determination of the shape, morphological and wettability properties of quartz and their correlations. Minerals Engineering. 2003;**16**: 951-964. DOI: 10.1016/j.mineng.2003.07.002

[20] Koh PTL, Hao FP, Smith LK, Chau TT, Bruckard WJ. The effect of particle shape and hydrophobicity in flotation. International Journal of Mineral Processing. 2009;**93**:128-134. DOI: 10.1016/j.minpro.2009.07.007

[21] Verrelli DI, Bruckard WJ, Koh PTL, Schwarz MP, Follink B. Particle shape effects in flotation. Part 1: Microscale experimental observations. Minerals Engineering. 2014;**58**: 80-89. DOI: 10.1016/j.mineng.2014.01.004

[22] Xia WC. Role of particle shape in the floatability of mineral particle: An overview of recent advances. Powder Technology. 2017;**317**:104-116. DOI: 10.1016/j.powtec.2017.04.050

[23] Feng D, Aldrich C. A comparison of the flotation of ore from the Merensky reef after wet and dry grinding. International Journal of Mineral Processing. 2000;**60**:115-129. DOI: 10.1016/S0301-7516(00)00010-7

[24] Zhu GL, Wang YH, Liu XW, Yu FS, Lu DF. The cleavage and surface properties of wet and dry ground spodumene and their flotation behavior. Applied Surface Science. 2015; **357**:333-339. DOI: 10.1016/j.apsusc.2015.08.257

[25] Xu LH, Hu YH, Wu HQ, Tian J, Liu J, Gao ZY, Wang L. Surface crystal chemistry of spodumene with different size fractions and implications for flotation. Separation and Purification Technology. 2016;**169**:33-42. DOI: 10.1016/j.seppur.2016.06.005

[26] Ilhan S, Kalpakli AO, Kahruman C, Yusufoglu I. The investigation of dissolution behavior of gangue materials during the dissolution of scheelite concentrate in oxalic acid solution. Hydrometallurgy. 2013;**136**:15-26. DOI: 10.1016/j.hydromet.2013.02.013

[27] Gao ZY, Bai D, Sun W, Cao XF, Hu YH. Selective flotation of scheelite from calcite and fluorite using a collector mixture. Minerals Engineering. 2015;**72**:23-26. DOI: 10.1016/j.mineng.2014.12.025

[28] Gao ZY, Sun W, Hu YH. New insights into the dodecylamine adsorption on scheelite and calcite: An adsorption model. Minerals Engineering. 2015;**79**:54-61. DOI: 10.1016/j.mineng.2015.05.011

[29] Cooper TG, de Leeuw NH. A combined ab initio and atomistic simulation study of the surface and interfacial structures and energies of hydrated scheelite: Introducing a CaWO4 potential model. Surface Science. 2003;**531**:159-176. DOI: 10.1016/S00039-6028(03)00362-5

[30] Deng LQ, Zhao G, Zhong H, Wang S, Liu GY. Investigation on the selectivity of N-((hydroxyamino)-alkyl) alkylamide surfactants for scheelite/calcite flotation separation. Journal of Industrial and Engineering Chemistry. 2016;**33**:131-141. DOI: 10.1016/j.jiec.2015.09.027

[31] Wang JJ, Gao ZY, Gao YS, Hu YH, Sun W. Flotation separation of scheelite from calcite using mixed cationic/anionic collectors. Minerals Engineering. 2016;**98**:261-263. DOI: 10.1016/j.mineng.2016.09.006

[32] Han HS, Hu YH, Sun W, Li XD, Cao CG, Liu RQ, Yue T, Meng XS, Guo YZ, Wang JJ, Gao ZY, Chen P, Huang WS, Liu J, Xie JW, Chen YL. Fatty acid flotation versus BHA flotation of tungsten minerals and their performance in flotation practice. International Journal of Mineral Processing. 2017;**159**:22-29. DOI: 10.1016/j.minpro.2016.12.006

[33] Yue T, Han HS, Hu YH, Sun W, Li XD, Liu RQ, Gao ZY, Wang L, Chen P, Zhang CY, Tian MJ. New insights into the role of Pb-BHA complexes in the flotation of tungsten minerals. Journal of Metals. 2017;**69**:2345-2351. DOI: 10.1007/s11837-017-2531-3

[34] Rupp F, Gittens RA, Scheideler L, Marmur A, Boyan BD, Schwartz Z, Geis-Gerstorfer J. A review on the wettability of dental implant surfaces I: Theoretical and experimental aspects. Acta Biomaterialia. 2014;**10**:2894-2906. DOI: 10.1016/j.actbio.2014.02.040

[35] Baek Y, Kang J, Theato P, Yoon J. Measuring hydrophilicity of RO membranes by contact angles via sessile drop and captive bubble method: A comparative study. Desalination. 2012;**303**:23-28. DOI: 10.1016/j.desal.2012.07.006

[36] Galet L, Patry S, Dodds J. Determination of the wettability of powders by the Washburn capillary rise method with bed preparation by a centrifugal packing technique. Journal of Colloid and Interface Science. 2010;**346**:470-475. DOI: 10.1016/j.jcis.2010.02.051

[37] Williams M, Fuerstenau D. A simple flotation method for rapidly assessing the hydrophobicity of coal particles. International Journal of Mineral Processing. 1987;**20**:153-157

[38] Yarar B, Kaoma J. Estimation of the critical surface tension of wetting of hydrophobic solids by flotation. Colloids and Surfaces. 1984;**11**:429-436

[39] Hu YH, Gao ZY, Sun W, Liu XW. Anisotropic surface energies and adsorption behaviors of scheelite crystal. Colloid Surface A. 2012;**415**:439-448. DOI: 10.1016/j.colsurfa.2012. 09.038

[40] Gao ZY, Sun W, Hu YH. Mineral cleavage nature and surface energy: Anisotropic surface broken bonds consideration. Transactions of Nonferrous Metals Society of China. 2014;**24**: 2930-2937. DOI: 10.1016/S1003-6326(14)63428-2

[41] Han HS, Liu WL, Hu YH, Sun W, Li XD. A novel flotation scheme: Selective flotation of tungsten minerals from calcium minerals using Pb-BHA complexes in Shizhuyuan. Rare Metals. 2017;**36**:533-540. DOI: 10.1007/s12598-017-0907-8

[42] Ulusoy U, Kursun I. Comparison of different 2D image analysis measurement techniques for the shape of talc particles produced by different media milling. Minerals Engineering. 2011;**24**:91-97. DOI: 10.1016/j.mineng.2010.05.011

[43] Ulusoy U, Yekeler M. Dynamic image analysis of calcite particles created by different mills. International Journal Of Mineral Processing. 2014;**133**:83-90. DOI: 10.1016/j.minpro. 2014.10.006

[44] Morgan DJ, Jerram DA. On estimating crystal shape for crystal size distribution analysis. Journal of Volcanology and Geothermal Research. 2006;**154**:1-7. DOI: 10.1016/j.jvolgeores. 2005.09.016

[45] Mock A, Jerram DA. Crystal size distributions (CSD) in three dimensions: Insights from the 3D reconstruction of a highly porphyritic rhyolite. Journal of Petrology. 2005;**46**:1525-1541. DOI: 10.1093/petrology/egi024

[46] Berger A, Herwegh M, Schwarz JO, Putlitz B. Quantitative analysis of crystal/grain sizes and their distributions in 2D and 3D. Journal of Structural Geology. 2011;**33**:1751-1763. DOI: 10.1016/j.jsg.2011.07.002

[47] Jerram DA, Mock A, Davis GR, Field M, Brown RJ. 3D crystal size distributions: A case study on quantifying olivine populations in kimberlites. Lithos. 2009;**112**:223-235. DOI: 10.1016/j.lithos.2009.05.042

[48] Gao ZY, Sun W, Hu YH, Liu XW. Surface energies and appearances of commonly exposed surfaces of scheelite crystal. Transactions of Nonferrous Metals Society of China. 2013;**23**:2147-2152. DOI: 10.1016/S1003-6326(13)62710-7

[49] Mogilevsky P, Parthasarathy TA, Petry MD. Anisotropy in room temperature micro-hardness and fracture of CaWo(4) scheelite. Acta Materialia. 2004;**52**:5529-5537. DOI: 10.1016/j.actamat.2004.08.022

[50] Mogilevsky P. Identification of slip systems in CaWO4 scheelite. Philosophical Magazine. 2005;**85**:3511-3539. DOI: 10.1080/14786430500227996

[51] Longo VM, Gracia L, Stroppa DG, Cavalcante LS, Orlandi M, Ramirez AJ, Leite ER, Andres J, Beltran A, Varela JA, Longo E. A joint experimental and theoretical study on the nanomorphology of $CaWO_4$ crystals. Journal of Physical Chemistry C. 2011;**115**: 20113-20119. DOI: 10.1021/jp205764s

[52] Li HL, Li TD, Liu HX, Huang BB, Zhang Q. Hierarchical flower-like nanostructures of anatase TiO_2 nanosheets dominated by {001} facets. Journal of Alloys and Compounds. 2016;**657**:1-7. DOI: 10.1016/j.jallcom.2015.09.257

[53] Gao ZY, Li CW, Sun W, Hu YH. Anisotropic surface properties of calcite: A consideration of surface broken bonds. Colloid Surface A. 2017;**520**:53-61. DOI: 10.1016/j.colsurfa.2017. 01.061

[54] Gao Z, Hu Y, Sun W, Drelich JW. Surface-charge anisotropy of scheelite crystals. Langmuir. 2016;**32**:6282-6288. DOI: 10.1021/acs.langmuir.6b01252

[55] Cebeci Y, Sonmez I. A study on the relationship between critical surface tension of wetting and oil agglomeration recovery of calcite. Journal of Colloid and Interface Science. 2004;**273**:300-305. DOI: 10.1016/j.jcis.2004.01.032

[56] Gao YS, Gao ZY, Sun W, Hu YH. Selective flotation of scheelite from calcite: A novel reagent scheme. International Journal of Mineral Processing. 2016;**154**:10-15. DOI: 10.1016/ j.minpro.2016.06.010